International Journal of Fracture **125:** 249–261, 2004.

Calculation of the energy J-integral for bodies with notches and cracks

YU.G. MATVIENKO[1,*] and E.M. MOROZOV[2]
[1]*Mechanical Engineering Research Institute of the Russian Academy of Sciences, 4 M. Kharitonievsky Per., 101990 Moscow, Russia (e-mail: matvienko7@yahoo.com)*
[2]*Moscow State Engineering Physics Institute - Technical University, 31 Kashirskoe Shosse, 115409 Moscow, Russia*

Received 25 March 2003; accepted in revised form 25 November 2003

Abstract. The approximate solutions for calculation of the energy J-integral of a body both with a notch and with a crack under elastic-plastic loading have been obtained. The crack is considered as the limit case of a sharp notch. The method is based on stress concentration analysis near a notch/crack tip and the modified Neuber's approach. The HRR-model and the method based on an equation of equilibrium were also employed to calculate the J-integral. The influence of the strain hardening exponent on the J-integral is discussed. New aspects of the two-parameter J_c^*-fracture criterion for a body with a short crack are studied. A theoretical investigation of the effect of the applied critical stress (or the crack length) on the strain fields ahead of the crack tip has been carried out.

Key words: elastic-plastic strain fields, HRR model, J-integral, notch, short and long cracks, two-parameter fracture criterion.

1. Introduction

Modern engineering structures made of materials with high toughness and low strength contains the stress concentration locations, such as notches, holes, cracks, etc. Loading of these structures is usually accompanied by plastic deformation in the neighborhood of stress concentration. Therefore, a description of the inelastic stress-strain fields ahead of a notch/crack tip and calculation of fracture mechanics parameters are necessary to estimate the behavior of a crack and structural integrity. As a result, models and criteria of elastic-plastic (nonlinear) fracture mechanics are needed to obtain realistic assessment of fracture process of damaged structures. Moreover, as a finite notch radius is introduced, a notch problem is much more complicated than a crack problem (e.g., W. Guo, 2002). Theoretical studies of elastic-plastic notch fields and fracture mechanics parameters are mainly limited to some simple cases.

Fracture mechanics parameters and criteria can be based on various elastic-plastic models of a solid. The energy J-integral is the most appropriate and commonly used elastic-plastic fracture parameter for description of the local elastic-plastic fields in the neighborhood of stress concentration and for study of crack initiation and propagation. The evaluation of the J-integral can be performed by numerical analysis and engineering estimation method. Normally, numerical investigation has been based on elastic-plastic finite element method (e.g., Atluri, 1985; Anderson, 1995; Rahman, 2001), elastic-plastic boundary element method (e.g., Cisilino and Aliabadi, 1999). These methods allow calculating the J-integral for any

*Author to whom correspondence should be addressed

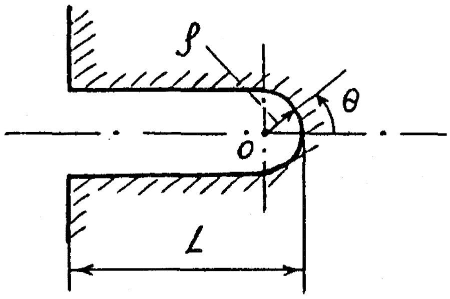

Figure 1. Geometry of a notch.

crack and body configuration and type of loading. The application of numerical methods in fracture mechanics makes it possible to analyze elastic-plastic stress and strain fields in the vicinity of any stress concentrator. However, the numerical analysis is enough expensive and time-consuming to be used routinely in engineering calculations. Other problem is that these numerical solutions are difficult to transfer from one body configuration or the material to another.

At the same time, number of analytical elastic-plastic solutions for the estimation of the stress concentration effect for bodies with different geometries is limited. Therefore, simplified estimation approach for engineering calculations has to be developed to predict the J-integral from viewpoint of elastic-plastic fracture theory. That is why the development of approximate methods for the analysis of elastic-plastic bodies with a stress concentrator is an important engineering problem.

The estimation technique consists of approximate J-integral equations as a function of applied load, crack size, mechanical properties of the material and geometry of structure (e.g., Kumar, German and Shih, 1981; Matvienko, 1994; Rahman and Brust, 1997; Schwalbe and Zerbst, 2000). The structural integrity assessment procedure (SINTAP) may be also regarded as an approximate J estimation technique (e.g., Webster and Bannister, 2000).

The focus of this study is to find simple procedures for the computation of the equations for $\boldsymbol{J}$-integral to reduce the need for finite element method calculations. New estimation methods have been developed to predict the J-integral of a body either with a notch or with a crack. The methods are based on stress concentration analysis and the method of sections. Possible application of the obtained formulas to analyze bodies of different geometries (including a crack emanating from the stress concentrator), the critical state of a body with a short crack and to estimate the stress and strain fields ahead of the short crack tip.

2. Calculation of the *J*-integral for a body with a notch

A body with a notch under a remotely applied tensile stress σ is considered. A notch with the curvature radius $\boldsymbol{\rho}$ at the tip has flat surfaces parallel to the χ axis (Figure 1). To estimate the stress and strain concentration, the energy J-integral suggested by Cherepanov (1979) and Rice (1968) bas been employed. The integration path is the contour of the notch tip, which is freed of stress. In this case, the $\boldsymbol{J}$-integral can be represented by the following simple expression

$$J = \int_{-\pi/2}^{\pi/2} W(\theta)\rho \cos\theta \, d\theta \tag{1}$$

Here $\boldsymbol{W}(\theta)$ is the density of strain energy and $\boldsymbol{\theta}$ is the angular coordinate of points on the notch contour in the polar coordinate system (the pole is the center of the notch tip circle). It is assumed as a first approximation that the distribution of the density of strain energy on the surface of the notch tip arc can be estimated as

$$W = W_{\max} \cos\theta. \tag{2}$$

Then, the $\boldsymbol{J}$-integral given by Equation (1) is rewritten in the form

$$J = \frac{\pi}{2} W_{\max} \rho. \tag{3}$$

It was shown (Hajinski, 1983) that exact solutions of the stress intensity factor for typical cases of loading follow from Equation (3).

The maximum of the density of strain energy $\boldsymbol{W}_{\max}$ in Equation (3) can be written as $\int \sigma_i d\varepsilon_i$. If $\varepsilon_{i\max} \geq \varepsilon_0$ and the stress state is uniaxial, the value of $\boldsymbol{W}_{\max}$ for strain hardening materials is obtained as follows

$$W_{\max} = \int_0^{\varepsilon_0} \sigma_i d\varepsilon_i + \int_{\varepsilon_0}^{\varepsilon_{i\max}} \sigma_i d\varepsilon_i = \frac{\sigma_0^2}{2E} + \frac{\sigma_*}{1+m}\left(\varepsilon_{i\max}^{1+m} - \varepsilon_0^{1+m}\right), \tag{4}$$

where $\varepsilon_{\max}$ is the maximum local strain on the notch tip surface. The stress is related to strain for the elastic-plastic material by

$$\begin{aligned} \sigma_i &= E\varepsilon_i, \quad \sigma_i < \sigma_0 \\ \sigma_i &= \sigma_* \varepsilon_i^m, \quad \sigma_i \geq \sigma_0, \end{aligned} \tag{5}$$

where $\sigma_* = (\alpha\sigma_0)/\varepsilon_0^m$; m is the strain hardening exponent and $\boldsymbol{\alpha}$ is the constant value; $\varepsilon_0 = \sigma_0/E$; E is the Young's modulus; σ_0 is the yield stress. The index i denotes the stress and strain intensity. Substituting Equation (4) into Equation (3) leads to the following equation

$$J = \frac{\pi}{2}\rho\left[\frac{\sigma_0^2}{2E} + \frac{\sigma_*}{1+m}\left(\varepsilon_{i\max}^{1+m} - \varepsilon_0^{1+m}\right)\right]. \tag{6}$$

This expression allows finding the maximum intensity of strain and stress intensity on the surface of the notch tip using the radius of curvature, the mechanical properties and the energy $\boldsymbol{J}$-integral determined either experimentally or theoretically.

The right hand-side of Equation (6) can be defined in terms of stress and strain concentration factors. The stress and strain intensity concentration factors ahead of the notch tip at $\theta = 0$ are represented as follows

$$K_\varepsilon = \frac{\varepsilon_{i\max}}{\varepsilon_i}, \quad K_\sigma = \frac{\sigma_{i\max}}{\sigma_i}, \tag{7}$$

where ε_i and σ_i are the applied stress and strain intensities. Taking into account Equations (5) and (7), Equation (6) can be rewritten in the following form

$$J = \frac{\pi}{2}\rho \begin{cases} \dfrac{\sigma_0^2}{2E} + \dfrac{\sigma_*}{1+m}\left[\dfrac{\sigma_i^2}{\sigma_* E} K_\varepsilon K_\sigma - \left(\dfrac{\sigma_0}{E}\right)^{1+m}\right], & \dfrac{1}{K_t} \leq \dfrac{\sigma_i}{\sigma_0} < 1 \\ \dfrac{\sigma_0^2}{2E} + \dfrac{\sigma_*}{1+m}\left[\left(\dfrac{\sigma_i}{\sigma_*}\right)^{(1+m)/m} K_\varepsilon K_\sigma - \left(\dfrac{\sigma_0}{E}\right)^{1+m}\right], & \dfrac{\sigma_i}{\sigma_0} \geq 1 \end{cases} \tag{8}$$

It is assumed that the material is plastically deformed in the neighborhood of stress concentration, whereas the applied stress intensity σ_i can be either below or above the yield stress.

The Neuber's formula modified by Makhutov (1981) (see also Makhutov, Matvienko and Chernyakov, 1993) for the elastic-plastic deformation of the material in the neighborhood of stress concentration is used to eliminate the term of $\boldsymbol{K_\varepsilon K_\sigma}$ from Equation (8)

$$\frac{K_\varepsilon K_\sigma}{K_t^2} = F, \tag{9}$$

where

$$F = F(K_t, \overline{\sigma_i}, m) = (K_t\overline{\sigma_i})^{-n(1-m)[1-(\overline{\sigma_i}-1/K_t)]}.$$

Here, $\overline{\sigma_i} = \sigma_i/\sigma_0$, K_t is the theoretical stress concentration factor and n is a function of K_t and $\overline{\sigma_i}$. The value of n is usually considered as a constant equal to 0.5.

Taking into account Equations (8) and (9), the following equations have been obtained. In the initial stage of elastic-plastic deformation ahead of the notch tip for $1/K_t \le \overline{\sigma_i} < 1$, the $\boldsymbol{J}$-integral is determined by

$$J = \frac{\pi}{2}\rho\left\{\frac{\sigma_0^2}{2E} + \frac{\sigma_*}{1+m}\left[\frac{\sigma_i^2}{\sigma_* E}K_t^2 F - \left(\frac{\sigma_0}{E}\right)^{1+m}\right]\right\}. \tag{10}$$

In the stage of deformation for $\overline{\sigma_i} \ge 1$, Equation (8) can be rewritten in the following form

$$J = \frac{\pi}{2}\rho\left\{\frac{\sigma_0^2}{2E} + \frac{\sigma_*}{1+m}\left[\left(\frac{\sigma_i}{\sigma_*}\right)^{(1+m)/m} K_t^2 F - \left(\frac{\sigma_0}{E}\right)^{1+m}\right]\right\}. \tag{11}$$

The J-integral has been investigated as a function of the applied stress and the strain hardening exponent. It is attractive to use the normalized value of J/J_e, where $J_e = (\pi\rho K_t^2/4E)\sigma_i^2$ is the elastic component of the $\boldsymbol{J}$-integral ($\overline{\sigma_i} < 1/K_t$). The empirical constant of the material α is taken equal to 1. Then, Equations (10) and (11) lead to

$$\frac{J}{J_e} = \frac{1}{(K_t\overline{\sigma_i})^2}\left(1 - \frac{2}{1+m}\right) + \frac{2F}{1+m} \tag{12}$$

for $1/K_t \le \overline{\sigma_i} < 1$ and

$$\frac{J}{J_e} = \frac{1}{(K_t\overline{\sigma_i})^2}\left(1 - \frac{2}{1+m}\right) + \frac{2F}{(1+m)(\overline{\sigma_i})^{(m-1)/m}} \tag{13}$$

for $\overline{\sigma_i} \ge 1$.

The tendency of the value of J/J_e as the function of $\overline{\sigma_i}$, m and $K_t (n = 0.5)$ is shown in Figure 2. The normalized $\boldsymbol{J}$-integral increases with increasing $\overline{\sigma_i}$ and ability of the material to be deformed plastically (i.e., with the decrease of m). The value of J/J_e is weakly dependent on the stress concentration factor K_t. The $\boldsymbol{J}$-integral is equal to the elastic component J_e for $\overline{\sigma_i} < 1/K_t$. In the applied stress range $1/K_t \le \overline{\sigma_i} < 1$, the $\boldsymbol{J}$-integral is approximately constant value (close to J_e) and not greatly depended on $\overline{\sigma_i}$. The value of $\boldsymbol{J}$ increases when the applied stress exceeds the yield stress.

The calculation of the $\boldsymbol{J}$-integral for the case of a body with a notch and a crack emanating from it has also been analyzed (Figure 3). The crack is assumed to be short; i.e. the crack length l is less than the radius of curvature ρ of the notch. Therefore, such crack is placed in the

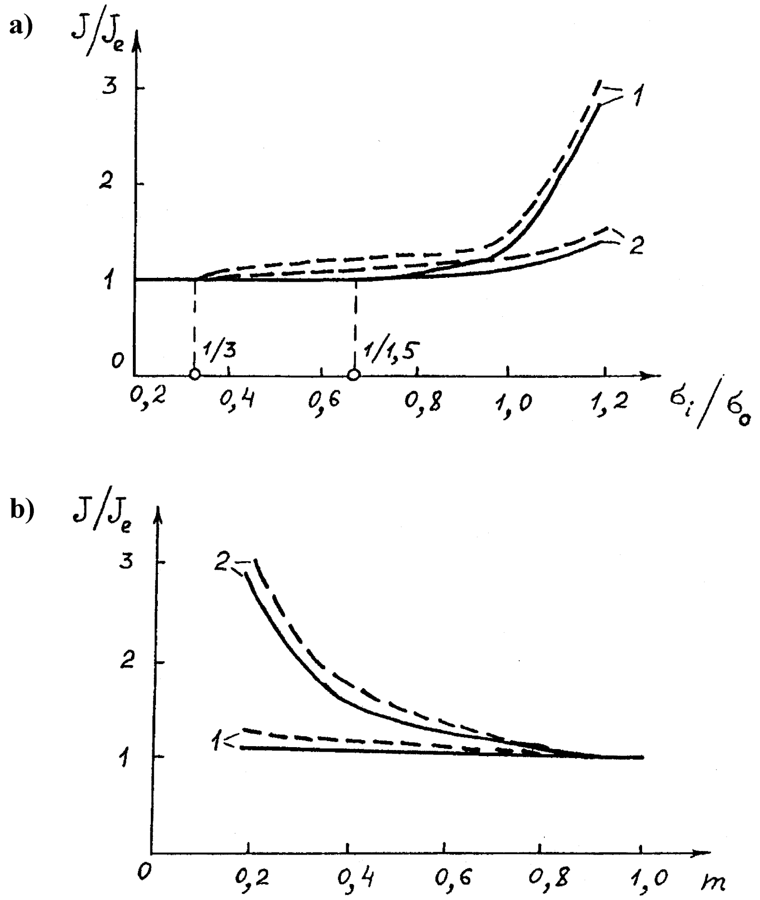

Figure 2. The normalized J-integral for a body with a notch. (a) Dependence of J/J_e on the applied stress: $1 - m = 0.2$, $2 - m = 0.5$. (b) Dependence of J/J_e on the hardening: $1 - \overline{\sigma_i} = 0.8$, $2 - \overline{\sigma_i} = 1.2$. Solid line - $K_t = 1.5$; dashed line - $K_t = 3$.

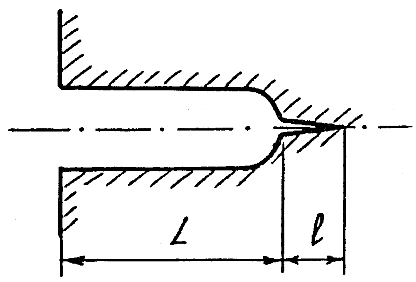

Figure 3. Geometry of a notch with a small crack.

'shadow' of the local stress peak due to the concentration ahead of the notch tip. Considered crack is intermediate between an 'infinitely long' crack (the concentration factor is equal to $K_{t\infty} = \sqrt{1 + (L/l)}$, where L is the notch length) and an 'infinitely short' crack (the concentration factor is equal to the theoretical stress intensity factor of a body with a notch K_t). In this case, the interpolation Neuber's method, which was successfully used by Hajinski (1983), can be employed. According to this method, the following stress concentration factor

$$K_{t^*} = 1 + \left[\frac{(K_t - 1)^2 (K_{t\infty} - 1)^2}{(K_t - 1)^2 + (K_{t\infty} - 1)^2} \right]^{1/2} \tag{14}$$

must be used in Equations (10) and (11) to calculate the $\boldsymbol{J}$-integral of a body with the notch and crack.

3. Calculation of *J*-integral for a body with a crack

The crack is assumed to be interpreted as a thin notch. In the limit case $\rho \to 0$, the notch is transformed into a crack, and Equations (10) and (11) give the expression for the $\boldsymbol{J}$-integral of a body with a crack-type notch

$$J = \begin{cases} \lim\limits_{\rho \to 0} \dfrac{\pi \rho K_t^2 F}{2(1+m)} \dfrac{\sigma_i^2}{E}, & \dfrac{1}{K_t} \le \overline{\sigma_i} < 1 \\ \lim\limits_{\rho \to 0} \dfrac{\pi \rho K_t^2 F \sigma_*}{2(1+m)} \left(\dfrac{\sigma_i}{\sigma_*} \right)^{(1+m)/m}, & \overline{\sigma_i} \ge 1 \end{cases} \tag{15}$$

The limit value of F is expected to be equal to $\lim_{K_t \to \infty} F = 1$ (Matvienko and Morozov, 1994). It is also worth that $K = \lim_{\rho \to 0} \frac{1}{2} \sqrt{\pi \rho} K_t \sigma$. In the case of a uniaxial stress state, equation described above leads to the well-known expression of $\boldsymbol{J}$-integral in terms of the stress intensity factor K in the elastic region ($J = G = K^2/E, \overline{\sigma_i} < 1/K_t$). In the plastically deformed region ahead of the crack tip, the $\boldsymbol{J}$-integral in the form (15) is defined as

$$J = \begin{cases} \left(\dfrac{2}{1+m} \right) \dfrac{K^2}{E}, & \dfrac{1}{K} < \overline{\sigma_i} < 1 \\ \left(\dfrac{2}{1+m} \right) \dfrac{K^2}{\sigma_*} \left(\dfrac{\sigma_i}{\sigma_*} \right)^{(1-m)/m}, & \overline{\sigma_i} \ge 1 \end{cases} \tag{16}$$

It is necessary to pay attention to the fact that the range of the applied stress starts from 0 ($1/K_t \to 0$). Therefore, there is not the elastic state ahead of the crack tip at any value of $\overline{\sigma_i}$. This is realistic situation for the materials. That is why the traditionally used and introduced for elastic bodies formula $J = J_e = K^2/E$ is idealized.

The $\boldsymbol{J}$-integral estimation technique can be also based on the method of sections developed previously by Matvienko (1997). The approximate formula of the $\boldsymbol{J}$-integral for a plane with a crack length $2l$ under a remote stress σ (Figure 4) has been obtained using the equation of equilibrium. It is assumed that the force, that is not transmitted by the crack, is counterbalanced by the additional force of the stress concentration near the crack tip (the origin of coordinates is at the crack tip), i.e. the following equation ocurs

$$\int_0^a \sigma_y dx = \sigma l. \tag{17}$$

The stress σ_y and strain ε_y on the crack extension line for a strain hardening material are taken according to the HRR model (Hutchinson, 1968; Rice and Rosengren, 1968)

$$\begin{aligned} \sigma_y &= \sigma_* \left(\frac{J}{\sigma_* I_m x} \right)^{m/(1+m)} \tilde{\sigma}_y(0, m) \\ \varepsilon_y &= \left(\frac{J}{\sigma_* I_m x} \right)^{1/(1+m)} \tilde{\varepsilon}_y(0, m), \end{aligned} \tag{18}$$

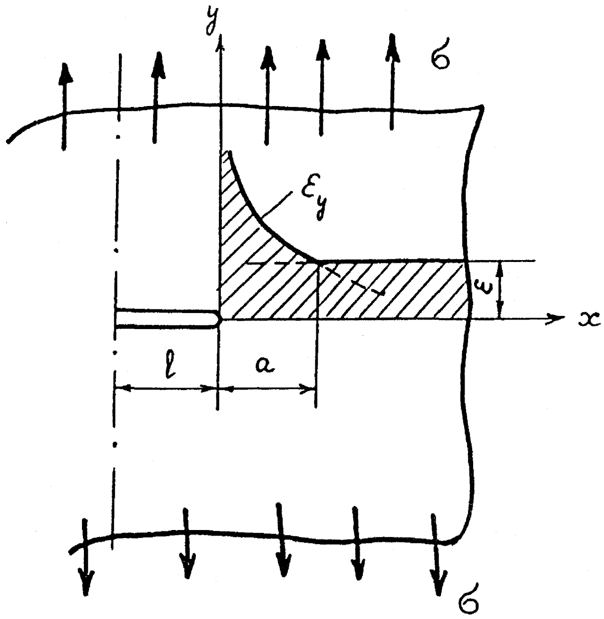

Figure 4. Distribution of the strain ahead of the crack tip on the line of crack extension in an infinite plate with a through crack.

where I_m is a undimensional value that depends on the stress state and the strain hardening exponent m; $\tilde{\sigma}_y(0, m)$ and $\tilde{\varepsilon}_y(0, m)$ are constant values. The length a is determined by the condition of equality of the strain ε_y (on the continuation of the crack) and the applied strain ε at the point $x = a$, i.e.

$$\begin{aligned} &\sigma_y = \sigma_* \left(\frac{\sigma}{E}\right)^m, \quad \sigma < \sigma_0 \\ &\sigma_y = \sigma, \qquad\qquad \sigma \geq \sigma_0 \end{aligned} . \tag{19}$$

These conditions allow writing the following equation

$$a = \begin{cases} \dfrac{J}{\sigma_* I_m}\left(\dfrac{E}{\sigma}\right)^{1+m} (\tilde{\sigma}_y(0, m))^{(1+m)/m}, & \sigma < \sigma_0 \\ \dfrac{J}{\sigma_* I_m}\left(\dfrac{\sigma_* \tilde{\sigma}_y(0, m)}{\sigma}\right)^{(1+m)/m}, & \sigma \geq \sigma_0 \end{cases} . \tag{20}$$

Using in the equation of balance (17), the stress σ_y in the form (18) and the value a according to Equation (20), approximate equations of the $\boldsymbol{J}$-integral become

$$J = \begin{cases} \dfrac{I_m}{(1+m)(\tilde{\sigma}_y(0, m))^{(1+m)/m}} \dfrac{\sigma^2 l}{E}, & \sigma < \sigma_0 \\ \dfrac{\sigma_* I_m}{1+m}\left(\dfrac{\sigma}{\sigma_* \tilde{\sigma}_y(0, m)}\right)^{(1+m)/m} l, & \sigma \geq \sigma_0 \end{cases} . \tag{21}$$

By substituting Equation (21) into Equation (20), the size of the region of strain concentration ahead of the crack tip is defined in the form

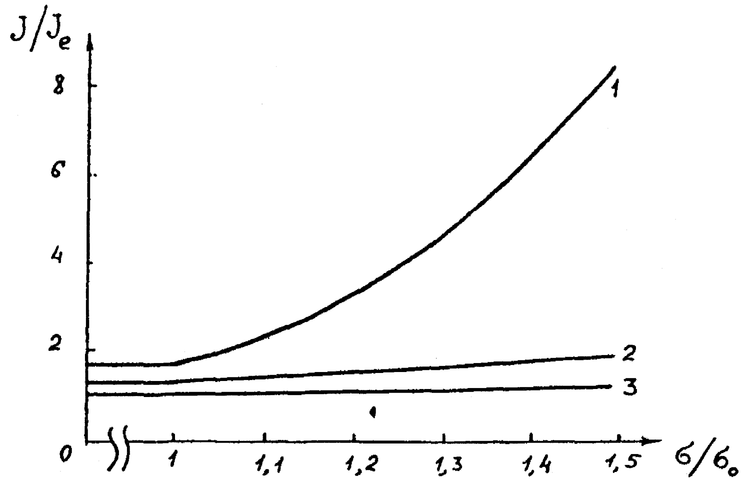

Figure 5. The energy $\boldsymbol{J}$-integral for a body with a crack: $1 - m = 0.2$, $2 - m = 0.5$, $3 - m = 0.8$.

$$a = \begin{cases} \dfrac{\sigma^{1-m}E^m}{\sigma_*(1+m)}l, & \sigma < \sigma_0 \\ \dfrac{l}{1+m}, & \sigma \geq \sigma_0 \end{cases}. \tag{22}$$

Therefore, in the case of the perfectly plastic and elastic materials, the value of a is determined from the following relations: $a = l$ for $m = 0$ and $a = 1/2$ for $m = 1$.

Manipulation of Equations (16) and (21), taking into account that $K = \sigma\sqrt{\pi l}$, shows that these equations of the $\boldsymbol{J}$-integral are fully compatible. Equation (16) at $\sigma_i \equiv \sigma$ can be rewritten in the following form

$$J = \begin{cases} \dfrac{2K^2}{(1+m)E}, & \dfrac{\sigma}{\sigma_0} < 1 \\ \dfrac{2K^2}{(1+m)\sigma_*}\left(\dfrac{\sigma}{\sigma_*}\right)^{(1-m)/m}, & \dfrac{\sigma}{\sigma_0} \geq 1 \end{cases}. \tag{23}$$

The tendency of J/J_e for a body with a crack is similar to that for a body with a notch (Figure 5). The value of J/J_e increases with the decrease of the strain hardening exponent and the increase of the applied stress. But in contrast to a body with a notch, the value of $J/J_e = 2/(1+m)$ is constant for a material with fixed m at the normalized applied stress $\sigma/\sigma_0 < 1$.

For other configuration of a body the stress intensity factor in Equation (23) must be written as $K = \sigma\sqrt{\pi l}Y$ taking into account the correction function Y.

Thus, Equation (23) obtained for calculation of the $\boldsymbol{J}$-integral allows the use of the energy $\boldsymbol{J}$-integral concept both in the experimental estimation of the fracture toughness of materials and in the analysis of structural integrity of structures, since it is enough to know the stress intensity factor, the applied load, the crack length and the mechanical properties of the material (E, σ_*, and m) to determine the value of $\boldsymbol{J}$.

4. The two-parameter J_c^*-fracture criterion

The evaluation of structural integrity and the fracture toughness, addressing brittle and ductile fracture, plastic collapse can be based on the failure assessment diagram or two-parameter fracture criteria (e.g., Webster and Bannister, 2000). In the failure assessment diagram approach, both the comparison of the crack driving force with the material's fracture toughness and with the plastic load limit analysis is performed at the same time. Therefore, two parameters are calculated. One parameter is normalized load ratio and the second is the normalized stress intensity factor. Above-mentioned approaches are valid both for significant plastic strain and small cracks and for small plastic strain and large cracks. The two-parameter fracture criteria are usually based on approximate account of the plastic state of the material ahead of the crack tip. In addition to the two-parameter criteria for bodies with cracks, it is worth the ultimate crack resistance (Morozov, 1999), the engineering treatment method (Schwalbe and Zerbst, 2000), different modifications of the R6 method (Ainsworth and et al., 2000; Budden et al., 2000; Motarjemi and Kocak, 2002) and others.

Here, the two-parameter energy fracture criterion proposed by Matvienko (1986) has been discussed. This criterion is based on the relation between the $\boldsymbol{J}$-integral and the strain on the surface of the notch (crack) tip and the cumulative damage law (Matvienko, 2002). In this case, a failure assessment diagram can be defined in terms of the critical $\boldsymbol{J}$-integral[1]

$$\left(\frac{\sigma_c}{\sigma_u}\right)^{1/m} - \left(\frac{\sigma_c}{\sigma_f}\right)^{1/m} + \left(\frac{J}{J_c}\right)^{1/(1+m)} = 1. \tag{24}$$

From this criterion the condition of fracture for a body with a finite crack can be represented in the form

$$J = J_c^*, \qquad J_c^* = J_c\left[1 - \lambda\left(\frac{\sigma_c}{\sigma_u}\right)^{1/m}\right]^{1+m}. \tag{25}$$

Here $\lambda = 1 - (\sigma_u/\sigma_f)^{1/m}$, σ_u is the ultimate strength, σ_f is the true ultimate strength and σ_c is the applied critical stress. In Equations (24) and (25) the critical value of the $\boldsymbol{J}$-integral (taking into account other criterion values) is denoted by the symbol $\boldsymbol{J}_c^*$. The $\boldsymbol{J}_c^*$-criterion (25) defines the failure assessment diagram, based on the $\boldsymbol{J}$-integral concept. The results of calculation of the normalized critical $\boldsymbol{J}_c^*$-integral are given in Figure 6.

The two-parameter $\boldsymbol{J}_c^*$-fracture criterion allows the analysis of influence of the strain hardening exponent m on the crack resistance of the material. For a linear elastic body with a crack ($m = 1$, $\sigma_u = \sigma_f$, $J_{(c)} \sim K_{(c)}^2$ independently on the critical stress), the criterion (25) gives Irwin's one-parameter force criterion of fracture $K = K_c$. For materials with the strain hardening exponent $0 < m \leq 0.3$ and $\sigma_f/\sigma_u \geq 2$, the coefficient λ that characterizes the material' s hardening tends to unit because the contribution of the term $(\sigma_u/\sigma_f)^{1/m}$ in λ is negligible, and the critical stress σ_c for a specimen with a crack of any size cannot exceed the ultimate strength σ_u. For plastic materials at $\lambda \neq 1$, the applied critical stress for a specimen (a structure) with a small (but finite) crack can exceed σ_u. In this case, the presence of the crack in the specimen does not lead to a decrease of the strength compared with a specimen without a crack (i.e., $\sigma_c \geq_{\sigma_u}$) if the following condition is met

$$J \leq J_c\left(\frac{\sigma_u}{\sigma_f}\right)^{(1+m)/m}. \tag{26}$$

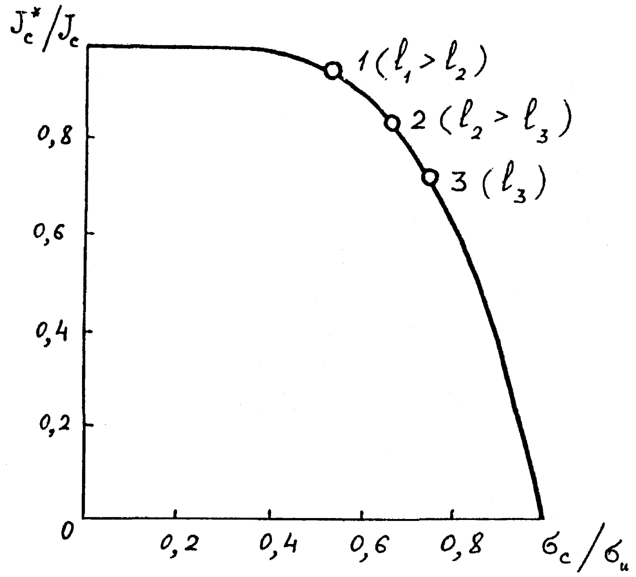

Figure 6. Critical values of the energy J-integral for 12X18H9T steel. The curve is drawn in accordance with Equation (25) at $m = 0.2$ and $\lambda \approx 1$.

Therefore, this approach allows determining the crack length that does not lead to the decrease of the specimen's strength, i.e. $\sigma_u \leq \sigma_c < \sigma_f$. The details of the criterion (25) and connection with other two-parameter fracture criteria have been discussed in Refs. (Matvienko, 1986; Makhutov and Matvienko, 1998). The approach based on the two-parameter J_c^*-fracture criterion can be also regarded as an approximate J estimation technique.

5. The strain fields ahead of the short crack tip

The analysis of the stress and strain fields ahead of the crack tip can be also based on the two-parameter J_c^*-fracture criterion. The energy J-integral is a function of the crack length, the applied stress, material properties and geometry of a body. Within the J_c^*-criterion the region of sufficiently small normalized critical stress σ_c/σ_c (or large cracks), in which the one-parameter fracture criterion $J = J_c^* = J_c$ is valid, can be determined (Figure 6). For such relatively long cracks, according to the HRR model, the elastic-plastic fracture toughness J_c characterizes the singular stress and strain fields ahead of the crack tip and controls the failure process both for small-scale and for large-scale yielding (Matvienko and Morozov, 1987; Kang and Kobayashi, 1988). At the same time, in the region of significant large stress σ_c/σ_u (short cracks) $J < J_c$ (points 2 and 3 in Figure 6); i.e., the one-parameter J_c criterion is supplemented by the criterion of maximal normal critical stress. Thus, the two-parameter fracture criterion in the form (25) is valid. How is changed the stress and strain field ahead of the crack tip in this case?

To answer this question, the HRR model has been extended to the critical state of a body with a short crack. It can be concluded that the value of J in Equation (18) is the right hand-side of the criterion relation (25), i.e., J_c^*. Therefore, the stress and strain distribution ahead of the crack tip at the moment of crack growth initiation (within the J_c^*-criterion) depends

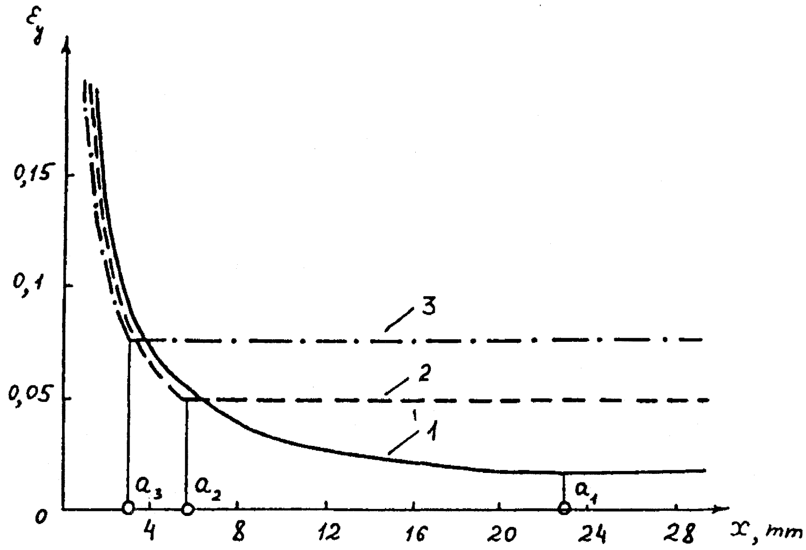

Figure 7. The strain distribution ahead of the crack tip for different lengths of critical crack. Lines 1, 2, 3 have the same notation as in Figure 6 and correspond to the different crack lengths $l = 27$, 6.6 and 3.6 mm. The segments of the χ axis $0 - a_i$ $(i = 1, 2, 3)$ represent the regions of significant strain gradient for different crack lengths.

not only on $\boldsymbol{J}_c$ and other mechanical properties of the material but also on the applied critical stress σ_c.

The size a of the zone, in which the singular stress and strain field is valid, is determined by Equation (22). These formulas show that the size of the singular strain zone decreases with decreasing crack length. The condition (22) can be considered as the boundary condition. On the basis of the HRR model [formulas (18)] and the $\boldsymbol{J}_c^*$-criterion (25), the strain ε_y ahead of the crack tip on the crack extension line is defined by the following

$$\varepsilon = \begin{cases} \left(\dfrac{J_c}{\sigma_* I_m \chi}\right)^{1/(1+m)} \tilde{\varepsilon}_y(0, m) \left[1 - \lambda \left(\dfrac{\sigma_c}{\sigma_u}\right)^{1/m}\right], & \chi < a \\ \varepsilon_c, & \chi \geq a, \end{cases} \tag{27}$$

where ε_c is the applied critical strain.

The results of the calculation of ε_y for a center cracked tension specimen of 12X18H9T stainless steel at $\theta = 0$ (Equation (27)) are given in Figure 7. The mechanical properties of the steel are the following: $J_c = 480$ MPa·mm, $m = 0.2$, $\sigma_* = 770$ MPa, $\sigma_0 = 340$ MPa, $\sigma_u = 620$ MPa, and $\sigma_f = 1600$ MPa. The calculation has been carried out for specimens with various crack lengths. The parameters of state are marked by points on the critical curve (Figure 6). Figure 7 shows that increasing the applied critical stress σ_c. (or decreasing the crack length l) leads to the decrease of the strain singular zone size and the increase of the remote strain component ε_c; i.e., 'spreading' of the strain gradient occurs. Therefore, the singular stress and strain fields of long cracks make a greater contribution in the whole picture of the stress and strain state ahead of the crack tip. For short cracks, the critical applied parameters of loading shade the singularity of the stress and strain fields ahead of the crack tip. This considerable role of critical stress and strain in formation of the stress and strain fields ahead of the short crack tip is supported by results of Makhutov and Domojirov (1989). It was shown that there is the effect of the regular terms of the stress tensor components on the size of the plastic zone.

6. Conclusions

Approximate $\boldsymbol{J}$-integral formulas of a body with a crack (notch) in terms of the stress intensity factor (or the theoretical stress concentration factor), the applied load, the crack length (or the radius of the notch), and the mechanical properties of the material have been obtained. The HRR-model and the method of sections were also employed to estimate the $\boldsymbol{J}$-integral of a body with a crack.

New aspects of the two-parameter $\boldsymbol{J}_c^*$-fracture criterion describing a failure assessment diagram of a body with long and short crack are discussed. The existences of small cracks, which do not lead to the decrease of a structural strength, are shown. The approach based on the two-parameter $\boldsymbol{J}_c^*$-fracture criterion can be also regarded as an approximate $\boldsymbol{J}$ estimation technique.

Within the $\boldsymbol{J}_c^*$-criterion and the HRR model, the stress and strain fields ahead of a short crack tip at a moment of the crack growth initiation is not only determined by the critical J-integral and other mechanical properties but it depends on the applied critical stress σ_c.

Acknowledgements

The present research was carried out with the financial support of grant no. 01-01-00503 'Investigation of non-linear criteria and termo-fatigue fracture' from the Russian Foundation of Fundamental Research.

Endnotes

[1]Energy strain interpretation of the criterion has the form: $\dfrac{\varepsilon_c}{\varepsilon_u} - \dfrac{\varepsilon_c}{\varepsilon_f} + \left(\dfrac{J}{J_c}\right)^{1/(1+m)} = 1$, where ε_u and ε_f are the ultimate and true ultimate critical strain, ε_c is the critical applied strain.

References

Ainsworth R.A., Bannister A.C. and Zerbst U. (2000) An overview of the European flaw assessment procedure SINTAP and its validation. *International Journal of Pressure Vessels and Piping* **77**, 869–876.

Anderson T.L. (1995) *Fracture Mechanics: Fundamentals and Applications*. CRC Press, Boca Raton.

Atluri S.N. (ed.) (1986) *Computational Methods in the Mechanics of Fracture*. North-Holland Publ. Co., Amsterdam, 430 pp.

Budden P.J., Sharples J.K. and Dowling A.R. (2000) The R6 procedure: resent developments and comparison with alternative approaches. *International Journal of Pressure Vessels and Piping* **77**, 895–903.

Cisilino A.P. and Aliabadi M.H. (1999) BEM implementation of the energy domain integral for the elastoplastic analysis of 3D fracture problems. *International Journal of Fracture* **96**, 229–245.

Cherepanov C.P. (1979) *Mechanics of Brittle Fracture*. McGraw-Hill, New York.

Guo W. (2002) Theoretical investigation of elastoplastic notch fields under triaxial stress constraint. *International Journal of Fracture* **115**, 233–249.

Hajinski G.M. (1983) Calculation of concentrators when elastic-plastic deforming. *Rastchety na Prochnost* **24**, 41–53 (in Russian).

Hutchinson W. (1968) Singular behavior of the end of a tensile crack in hardening materials. *Journal of Mechanics and Physics of Solids* **16**, 13–31.

Kumar V., German M.D. and Shih C.F. (1981) An Engineering Approach for Elastic-Plastic Fracture Analysis. Report EPRI NP-1931, Electric Power Research Institute, Palo Alto.

Makhutov N.A. (1981) *Deformation Criteria of Fracture and Calculation of Strength of Construction Element*. Mashinostroenie, Moscow (in Russian).

Makhutov N.A. and Domojirov L.1. (1989) Two-parameter failure criterion in view of refined size of plastic zone. *Zavodskaya Laboratoriya* **N 1** 54–59 (in Russian).

Makhutov N.A., Matvienko Yu.G. and Chernyakov S.V. (1993) A unified methodological approach to calculation analysis of the stages of nucleation and growth of low-cycle fatigue cracks. *Materials Science* **29**, 109–114.

Makhutov N.A. and Matvienko Yu.G. (1998) Fracture toughness characterization. In G.P. Cherepanov (ed.) *FRACTURE: A Topical Encyclopaedia of Current Knowledge*. Krieger Publ. Comp. Florida pp. 359–366.

Matvienko Yu.G. (1986) Two-parameter failure criterion and hardening of material. *Zavodskaya Laboratoriya* **N 9** 60–62 (in Russian).

Matvienko Yu.G. (1994) J-estimation formulas for non-linear crack problems. *International Journal of Fracture* **68**, R15–R18.

Matvienko Yu.G. (1997) Aproximate solution for hardening solids with a crack. In R.K. Mahidhara, A.B. Geltmacher, K. Sadananda and P. Matic (eds.) *Recent Advances in Fracture*. TMS publ. Warrendale pp. 307–313.

Matvienko Yu.G. (2002) Damage process and crack propagation in materials. In A. Neimitz, I.V. Rokach, D. Kocanda and R. Golos (eds.) *Proc. of the 14th European Conference on Fracture 'Fracture Mechanics beyond 2000'*. EMAS Publ., UK vol. 2, pp. 467–474.

Matvienko Yu.G. and Morozov E.M. (1987) Some problems in linear and non-linear fracture mechanics. *Engineering Fracture Mechanics* **28**, 127–138.

Matvienko Yu.G. and Morozov E.M. (1994) A method for approximate calculation of the energy integral for notched and cracked bodies. *Materials Science* **30**, 345–349.

Morozov E.M. (1999) An ultimate crack resistance concept. *Fatigue and Fracture of Engineering Materials and Structures* **22**, 997–1001.

Motarjemi A.K. and Kocak M. (2002) Fracture assessment of a clad steel using various SINTAP defect assessment procedure levels. *Fatigue and Fracture of Engineering Materials and Structures* **24**, 929–939.

Rahman S. (2001) Probabilistic fracture mechanics: J-estimation and finite element methods. *Engineering Fracture Mechanics* **68**, 107–125.

Rahman S. and Brust F.W. (1997) Approximate methods for predicting J-integral of a circumferentially surface-cracked pipe subject to bending. *International Journal of Fracture* **85**, 111–130.

Rang B.S.I. and Kobayashi A.S. (1988) J-estimation procedure based on Moire interferometry data. *Transaction of ASME, Journal of Pressure Vessel Technology* **110**, 291–300.

Rice J. (1968) A path-independent integral and the approximate analysis of strain concentration by notches and cracks. *Journal of Applied Mechanics* **35**, 379–386.

Rice J.R. and Rosengren G.F. (1968) Plane strain deformation near a crack tip in a power-law hardening materials. *Journal of Mechanics and Physics of Solids* **16**, 1–12.

Schwalbe K.-H. and Zerbst U. (2000) The engineering treatment model. *International Journal of Pressure Vessels and Piping* **77**, 905–918.

Webster S. and Bannister A. (2000) Structural integrity assessment procedure for Europe – of the SINTAP program overview. *Engineering Fracture Mechanics* **67**, 481–514.